

Video Figure S1

2014132\_KPgSurfaceFit.txt

**SUPPLEMENTAL METHODS****Stratigraphy**

We surveyed elevations at HCF-TUM contact localities using a high-precision Trimble 2005 GeoExplorer XT GPS receiver, and found that the contact is remarkably planar. The best-fit plane has a maximum residual of 8 m and RMSE of 3.7 m, just twice the instrumental precision of the GPS receiver (< 2 m). We used GPS receivers to acquire geographic coordinates for all fossil sampling localities, and projected those coordinates to the best-fit plane to determine the stratigraphic height of each locality relative to the HCF-TUM ( $\approx$  K-Pg boundary). These stratigraphic data were compared to previously published stratigraphic heights (Hartman, 1998; Wilson, 2005) and geologic maps (Wilde and Vuke, 2004a, 2004b; Wilde and Bergatino, 2004a, 2004b) for compatibility. Only two sites diverged by more than 5 m from published estimates. L0010a was projected to be 10 m above the K-Pg boundary, though Hartman (1998) recorded it as 35 m above the boundary. We accept the latter value, as there is clear exposure of 20–25 m of TUM below the fossil horizon, and projection at this site requires extrapolation of the best-fit plane beyond recorded data points. A NW-SE fault in the lower center of the map offsets localities L6214/5 (Site L)(Wilde and Vuke, 2004a). Wilde and Vuke (2004a) map the fault as having approximately 200 m of offset, consistent with the difference between published height estimates (Hartman, 1998) for that location and our projected height (195 m). Uncertainties on stratigraphic heights are a combination of GPS precision estimates (typically < 1.5 m) and uncertainties derived from stratigraphic projections (typically < 3.0 m). A copy of this model is available as a Matlab file (KPgSurfaceFit.m) with contained instructions that can be used to examine this surface model and find projected surface locations (and confidence intervals) for any geographical location. Details of each locality, including specific uncertainty estimates can be found in Table S1. In many cases, larger upper bounds on stratigraphic height were added to the analytical uncertainties to reflect shells being retrieved from the bottom of large channel structures that down cut into surrounding overbank deposits, and the corresponding uncertainty in the relative timing when compared to neighboring flat-lying deposits. We note that, despite large numbers of published sampling localities and considerable field exploration, bivalve fossils were absent from the lowest 30 m of the TUM.

**Laboratory Methods**

We collected unionid bivalve fossils from ten localities in the study area with the goal of even stratigraphic sampling of the HCF and TUM, although no bivalve fossil localities are known from the lowest 30 m of the TUM. We also sampled rarer gastropod fossils from two localities and carbonate vein material from one locality. To serve as a modern analog, we collected unionid bivalves from the Amite River, near Denham Springs, Louisiana. The temperature and depositional environment at this location approximate conditions during deposition of the HCF. Daily historical temperature records for the past 50 years are available from a USGS water-temperature monitoring station located 35 km upstream of this location and from an air temperature station located in nearby Baton Rouge, Louisiana (15 km).

We prepared three or four bivalve shells from each locality (fossil and modern) by drilling near the umbo of the shell to generate carbonate powder for analysis. The umbo is selected for two reasons, one practical, the other theoretical. Primarily the umbo serves as standardized location on each shell to minimize variations between sampled bivalves. Secondly, the umbo is selected because bivalves are likely to exhibit less seasonal bias early in their life due to the importance of constructing their initial shell for protection. Unfortunately, the results of this study revealed that seasonal bias was still present. This is particularly important because clumped isotope analysis currently requires almost two orders of magnitude more carbonate material than traditional isotopic techniques (Eiler, 2007), so our preparation technique was designed to average multiple years of growth instead of examining seasonal variability. We assessed diagenesis of visually pristine, fully aragonitic (as confirmed by XRD) material from bivalve shells using trace element concentrations (no correlations between either  $\delta^{18}\text{O}$  or  $\Delta 47$  with [Al], [Ba], [Fe], [Mn], [Na], [Sr] were found). Additionally, we sectioned and examined a subset of samples under cold-cathode cathodoluminescence (CL) microscopy; no bivalves were found to exhibit any signs of recrystallization. Under CL illumination, gastropod fossils showed textures and luminescence characteristic of diagenesis. Presumably recrystallized calcite was detected by XRD in primarily aragonitic gastropod sample powders, but not in primarily aragonitic bivalves.

Stable isotopic measurements were made in two batches at the California Institute of Technology (Caltech), the first in November 2010 and the second in February 2012. In both batches carbonate powders were reacted with 90 °C 100% phosphoric acid and the emitted CO<sub>2</sub> gas was purified through two cryogenic trap sequences separated by a He carried gas chromatograph transit before introduction to the sample bellows of Thermo MAT 253 mass spectrometer. Measurements were interspersed with internal lab standard carbonate powders, heated gases, and in the case of the later batch, low-temperature, water-equilibrated gases. Detailed laboratory methods follow supplemental information of Passey et al. (2010) and raw mass spectrometry data was processed as in Huntington et al. (2009), modified to convert measurements to absolute reference frame (Dennis et al., 2011). Analyses (6 of 145) with  $\Delta 48$  signatures indicative of methodological contamination ( $\Delta 48$  anomalies) were removed from the final compilation (Huntington et al., 2009), as were samples with anomalously high  $\Delta 47$  values (>1.0; n=2). Shells for which only one successful analysis (n=3) remained were excluded from the final data compilation (Table S2), but are included in the raw clumped isotope data (Table S3).

Each bivalve shell was analyzed either two or three times to generate mean shell values  $\Delta 47$  values, which were in turn averaged to generate mean locality  $\Delta 47$  values and uncertainty estimates. Corrected  $\Delta 47$  values in the absolute reference frame were converted to temperature using equation 7 from Zaarur et al. (2013). Formulae from Kim et al. (2007) and Kim and O'Neil (1997) were used to reconstruct  $\delta^{18}\text{O}_{\text{water}}$  from temperature and  $\delta^{18}\text{O}$  of the carbonate. The analyses and sample mean values of  $\Delta 47$  and  $\delta^{18}\text{O}_{\text{water}}$  can be found in Table S2. The net result of converting from the internal laboratory measurements to the absolute reference frame for the 2010 batch was a 1.5 °C increase in reconstructed temperature. While we use the most recent of the  $\Delta 47$ -temperature calibrations, other recent alternative calibrations have been proposed (Zaarur et al., 2011; 2013; Henkes et al., 2013; Eagle et al., 2013). In terms of absolute temperature estimates, these calibrations agree very well around 30 °C, but all have greater temperature sensitivities than the calibration we used, and would consequently show greater temperature changes. The aragonite calibrations from Eagle et al. (2013) and Henkes et al. (2013) have temperature sensitivities greater than the Zaarur calibration. While the Zaarur calibration yielded a 8 °C temperature decline (31-23 °C) that we use in the main text, using the alternative calibrations we would

reconstruct an 9 °C (34–23 °C) or a 13 °C (32–19 °C) decline using Eagle et al. (2013) or Henkes et al. (2013), respectively. We elected to use the Zaarur calibration because it is more conservative in estimated temperature changes, and the most recently published. Table S2 has the temperatures for the different calibrations identified for all analyses.

### Bimodality of $\delta^{18}\text{O}_{\text{water}}$

We observed that the  $\delta^{18}\text{O}_{\text{water}}$  was bimodally distributed, with values clustered around either -8‰ or -17‰, a pattern observed previously (Dettman and Lohmann, 2000; Fan and Dettman, 2009; Fricke et al., 2010). Several possible scenarios could explain this pattern, including differently sourced water (i.e. alpine v. lowland rainfall), different channel size, or monsoonal influence. We see no evidence in our field work for the second, and cannot differentiate between the first and last possibilities. Our primary concern is whether the different water types bias the temperature record, and there is no statistically significant relationship between temperature and  $\delta^{18}\text{O}_{\text{water}}$ . A *t*-test, designed to see whether two separate populations have statistically different means, was applied to the temperature values of the two  $\delta^{18}\text{O}_{\text{water}}$  populations, yielding a non-statistically significant result ( $p = 0.16$ ). There is at best a weak, non-significant, correlation ( $r^2 = 0.27$ ,  $p = 0.12$ ) between the two variables (Fig. S3) that, even if significant, would only explain 27% of the variation seen in the temperature values. Additionally, we also find for the two samples at the same stratigraphic height from different geographical localities (-66m, Fig. 2 of main text) that the temperatures are identical but differ in  $\delta^{18}\text{O}_{\text{water}}$ . The evidence suggests that there is little or no bias of temperature due to water source or channel effects.

### Works Cited in Supplemental Methods

- Dennis, K.J., Affek, H.P., Passey, B.H., Schrag, D.P., and Eiler, J.M., 2011, Defining an absolute reference frame for “clumped” isotope studies of CO<sub>2</sub>: *Geochimica et Cosmochimica Acta*, v. 75, p. 7117–7131.
- Dettman, D.L., and Lohmann, K.C., 2000, Oxygen isotope evidence for high-altitude snow in the Laramide Rocky Mountains of North America during the Late Cretaceous and Paleogene: *Geology*, v. 28, no. 3, p. 243–246.
- Eagle, R.A., Eiler, J.M., Tripati, A.K., Ries, J.B., Freitas, P.S., Hiebenthal, C., Wanamaker Jr., A.D., Taviani, M., Elliot, M., Marenssi, S.A., Nakamura, K., Ramirez, P., and Roy, K., 2013, The influence of temperature and seawater carbonate saturation state on <sup>13</sup>C-<sup>18</sup>O bond ordering in bivalve mollusks: *Biogeosciences Discussions*, v. 10, p. 157–194.
- Eiler, J.M., 2007, “Clumped-isotope” geochemistry—The study of naturally-occurring, multiply-substituted isotopologues: *Earth and Planetary Science Letters*, v. 262, no. 3-4, p. 309–327.
- Fan, M., and Dettman, D.L., 2009, Late Paleocene high Laramide ranges in northeast Wyoming: Oxygen isotope study of ancient river water: *Earth and Planetary Science Letters*, v. 286, no. 1-2, p. 110–121

Fastovsky, D.E., 1987, Paleoenvironments of vertebrate-bearing strata during the Cretaceous-Paleogene transition, eastern Montana and western North Dakota: *Palaios*, v. 2, p. 282–295, doi:10.2307/3514678.

Fricke, H.C., Foreman, B.Z., and Sewall, J.O., 2010, Integrated climate model-oxygen isotope evidence for a North American monsoon during the Late Cretaceous: *Earth and Planetary Science Letters*, v. 289, no. 1, p. 11–21.

Hartman, J.H., 1998, The biostratigraphy and paleontology of latest Cretaceous and Paleocene freshwater bivalves from the Western Williston Basin, Montana, USA: *Bivalves: an eon of evolution: Paleobiological studies honoring Norman D. Newell*, p. 317.

Henkes, G.A., Passey, B.H., Wanamaker, A.D., Grossman, E.L., Ambrose, W.G., and Carroll, M.L., 2013, Carbonate clumped isotope compositions of modern marine mollusk and brachiopod shells: *Geochimica et Cosmochimica Acta*, doi: <http://dx.doi.org/10.1016/j.gca.2012.12.020>.

Huntington, K.W., Eiler, J.M., Affek, H.P., Guo, W., Bonifacie, M., Yeung, L.Y., Thiagarajan, N., Passey, B., Tripati, A., Daëron, M., and Came, R., 2009, Methods and limitations of “clumped”  $\text{CO}_2$  isotope ( $\Delta 47$ ) analysis by as-source isotope ratio mass spectrometry: *Journal of Mass Spectrometry*, v. 44, no. 9, p. 1318–1329.

Kim, S.T., and O’Neil, J.R., 1997, Equilibrium and nonequilibrium oxygen isotope effects in synthetic carbonates: *Geochimica et Cosmochimica Acta*, v. 61, no. 16, p. 3461–3475.

Kim, S.T., Oneil, J., Hillairemarcel, C., and Mucci, A., 2007, Oxygen isotope fractionation between synthetic aragonite and water: Influence of temperature and  $\text{Mg}^{2+}$  concentration: *Geochimica et Cosmochimica Acta*, v. 71, no. 19, p. 4704–4715.

Passey, B.H., Levin, N.E., Cerling, T.E., Brown, F.H., and Eiler, J.M., 2010, High-temperature environments of human evolution in East Africa based on bond ordering in paleosol carbonates: *Proceedings of the National Academy of Sciences*, v. 107, no. 25, p. 11245–11249.

Wilde, E.M., and Bergatino, R.N., 2004a, Geologic map of the Fort Peck Lake East 30' x 60' quadrangle, eastern Montana: Montana Bureau of Mines and Geology, v. Open-File Report 498.

Wilde, E.M., and Bergatino, R.N., 2004b, Geologic map of the Fort Peck Lake West 30' x 60' quadrangle, eastern Montana: Montana Bureau of Mines and Geology, v. Open-File Report 499.

Wilde, E.M., and Vuke, S.M., 2004a, Geologic map of the Jordan 30' x 60' quadrangle, eastern Montana: Montana Bureau of Mines and Geology, v. Open-File Report 514.

Wilde, E.M., and Vuke, S.M., 2004b, Geologic map of the Sand Springs 30' x 60' quadrangle, eastern Montana: Montana Bureau of Mines and Geology, v. Open-File Report 515.

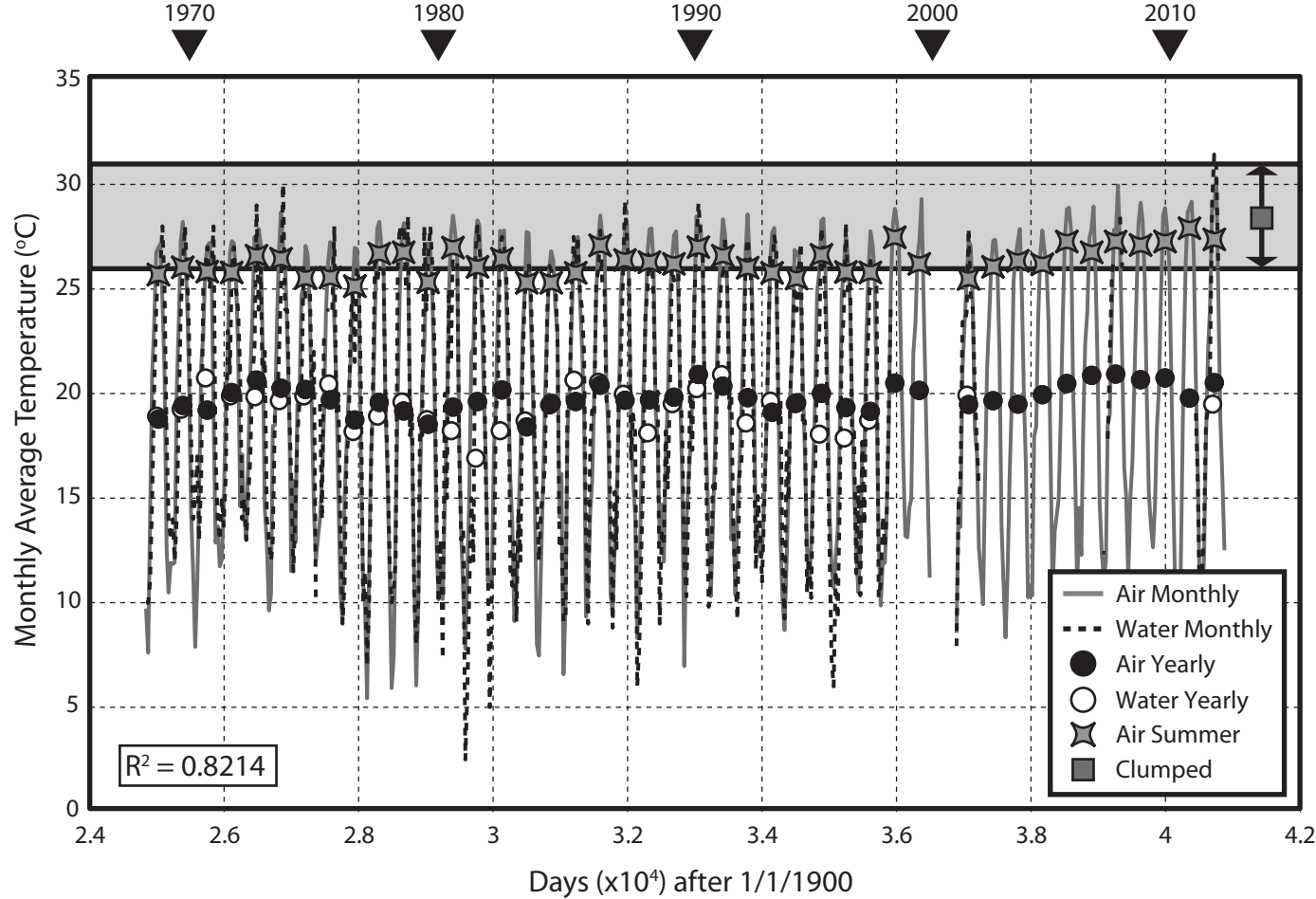
Zaarur, S., Olack, G., and Affek, H.P., 2011, Paleo-environmental implication of clumped isotopes in land snail shells: *Geochimica et Cosmochimica Acta*, v. 75, no. 22, p. 6859–6869.

## SUPPLEMENTARY FIGURE CAPTIONS

Figure DR1. Animated rotating image of HCF-TUM locality coordinates (green triangles) and the best-fit plane to the data. Red dots are fossil sampling locations, projected a distance along red lines to best-fit plane. ~200x vertical exaggeration.

Figure DR2. Monthly average air and water temperature records constructed from daily records for nearest monitored location to modern unionid bivalve sampling location (used as modern analog for fossil unionids). At far right: clumped isotope temperature with 95% confidence interval reconstructed for modern shells. Modern unionids grow primarily during summer months and record a summer average temperature.

Figure DR3. Bivalve  $\delta^{18}\text{O}_{\text{water}}$  plotted against reconstructed temperature with no statistically significant relationship.



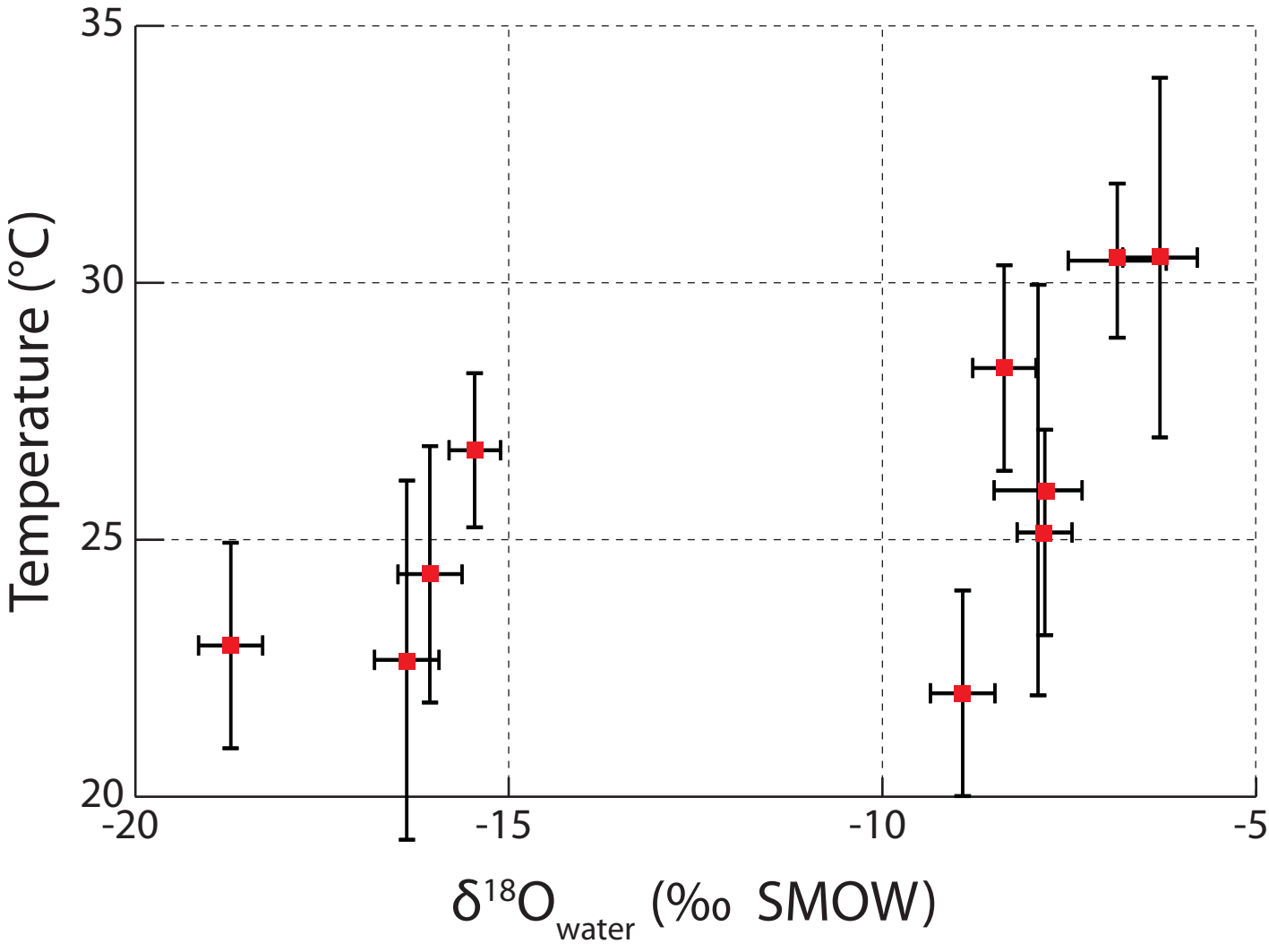


Table DR1. Sample Key for Figures MAP and RESIDUALS, GPS coordinates are available to qualified researchers - please contact one of the first two authors

<b>Letter</b>	<b>Type</b>	<b>Description</b>	<b>Strat and Uncertainty (<math>\pm</math> 95% analytical, -geological) m</b>	<b>Stratigraphic Height for Fossils</b>
A	K-Pg	near McKeever Ranch 1 (UCMP-V72210)		
B	K-Pg	near Billy Creek 1 (UCMP-V72211) & 2 (V75173)		
C	K-Pg (Impact evidence)	Iridium Hill (no Trimble GPS) see Alvarez (1983)		
D	K-Pg (Impact evidence)	near Herpjunk Promontory (UCMP-V77129)		
E	K-Pg (Impact evidence)	near Herpjunk Promontory (UCMP-V77129)		
F	K-Pg	near Hell's Hollow Channel (UCMP-V74110)		
G	Fossil Sample	L0019 - Hartman (1998)	-10.7 $\pm$ 3.0, -2	From Hartman (1998) - beyond areal extent of stratigraphic plane, though consistent with stratigraphic plane value (15m $\pm$ 18m)
H	Fossil Sample	MacDonald (UCMP-72201)	33.6 $\pm$ 3.3, -15	Stratigraphic plane assignment
I	K-Pg (Impact evidence)	Brownie Butte - see Bohor et al. (1984)		
J	K-Pg	Section G from Fastovsky (1987)		
K	Fossil Sample	L5233A - Hartman (1998)	-26.3 $\pm$ 2.8, -3	Stratigraphic plane assignment (matches Hartman 1998) From Hartman (1998) - fault offsets location from strat plane, location is also outside areal extent of stratigraphic plane - mapped fault offset matches strat plane offset within error
L	Fossil Sample	L6214 & L6215 - Hartman (1998)	-4.3/-1.5 $\pm$ 3.0, 0, L6214-L6215 stratigraphic distance fixed at 2.8m as measured in outcrop	Stratigraphic plane assignment
M	Fossil Sample	Happy Days	-65.4 $\pm$ 2.9, -1	
N	K-Pg (Impact evidence)	Lerbekmo Hill - see Baadsgaard et al. (1998)		
O	Fossil Sample	Gene Gastropod	-20.5 $\pm$ 2.6, 0	Stratigraphic plane assignment
P	Fossil Sample	near MicrotetonB (UWBM-C1165)	-66.0 $\pm$ 2.5, -6	Stratigraphic plane assignment
Q	K-Pg	near Broken Hart (UCMP-V82026)		
R	Fossil Sample	Shiny Things (UWBM-C1178)	-24.6 $\pm$ 3.6, -2.5	Stratigraphic plane assignment
S	K-Pg (Impact evidence)	Flag Butte - see Moore et al. (2014)		
T	Fossil Sample	near Harbaugh Ranch 1 (UWBM-C1420)	53.5 $\pm$ 11.6, -1	Stratigraphic plane assignment, outside areal extent of stratigraphic plane control, value matches within error with published geologic maps
U	K-Pg	Carl's Pile		
V	K-Pg	2 km from Yoshi's Microsite (UWBM-C1667)		
W	K-Pg	near Flat Creek 5 (UCMP-V73087)		

X Fossil Sample L0010a - Hartman (1998)

$35.4 \pm 3.0$ , -10

From Hartman (1998) - beyond  
strat. plane extent, geologic  
evidence on the ground contradicts  
theoretical strat. plane height

UCMP = University of California Museum of Paleontology

UWBM = University of Washington Burke Museum

Alvarez, L.W., 1983, Experimental evidence that an asteroid impact led to the extinction of many species 65 million years ago: Proceedings of the National Academy of Sciences of the United States of America, v. 80, no. 2, p. 627.

Baadsgaard, H., Lerbekmo, J.F., and McDougall, I., 1988, A radiometric age for the Cretaceous-Tertiary boundary based upon K-Ar, Rb-Sr, and U-Pb ages of bentonites from Alberta, Saskatchewan, and Montana: Canadian Journal of Earth Sciences, v. 25, no. 7, p. 1088–1097.

Bohor, B.F., Foord, E.E., Modreski, P.J., and Triplehorn, D.M., 1984, Mineralogic evidence for an impact event at the Cretaceous-Tertiary boundary: Science, v. 224, no. 4651, p. 867–869.

Fastovsky, D.E., 1987, Paleoenvironments of vertebrate-bearing strata during the Cretaceous-Paleogene transition, eastern Montana and western North Dakota: *Palaios*, p. 282–295.

Hartman, J.H., 1998, The biostratigraphy and paleontology of latest Cretaceous and Paleocene freshwater bivalves from the Western Williston Basin, Montana, USA: *Bivalves: an eon of evolution: paleobiological studies honoring Norman D. Newell*, p. 317.

Moore, J.R., Wilson, G.P., Sharma, M., Hallock, H.R., and Braman, D.R., 2014, Assessing the relationships of the Hell Creek-Fort Union contact, Cretaceous-Paleogene boundary, and Chicxulub impact ejecta horizon at the Hell Creek Formation lectostratotype, Montana, US: Geological Society of America Special Paper, v. 503, p. 123-136.

**Table DR2. Clumped Summary**

Analysis	Sample	Batch	Strat	d13C	d18o	ARF D47	se	T(Zaarur)	95%(from Gr)	95%sample(S)	d18Ow	d18Ow err	Eagle2013Ara	Eagle2013Bio	Henkes2013T	
2012_LA_1A_1		2		-8.84	-5.01	0.692	0.017	27.4			29.6	15.9	26.6			
2012_LA_1A_2		2		-8.82	-5.01	0.664	0.010	34.5			39.6	22.1	38.9			
2012_LA_1A_3	2012-LA-1A	2		-8.96	-4.90	0.698	0.012	26.1			27.7	14.7	24.4			
2012_LA_2A_1		2		-8.91	-4.71	0.710	0.013	23.2			23.7	12.1	19.6			
2012_LA_2A_2	2012-LA-2A	2		-7.47	-8.40	0.696	0.008	26.5			28.3	15.0	25.1			
2012_LA_3A_2		2		-8.84	-3.79	0.716	0.015	21.9			22.0	11.0	17.5			
2012_LA_3A_3		2		-8.78	-4.19	0.677	0.014	31.2			34.9	19.2	33.1			
2012_LA_3A_4	2012-LA-3A	2		-8.88	-4.15	0.699	0.012	25.9			27.5	14.5	24.1			
<b>Louisiana (Modern) Mean:</b>				<b>-8.63</b>	<b>-5.19</b>	<b>0.695</b>	<b>0.005</b>	<b>26.7</b>	<b>2.5</b>	<b>2.6</b>	<b>-3.2</b>	<b>0.4</b>	<b>28.8</b>	<b>15.3</b>	<b>25.7</b>	
HC_CC_A_1		2		-5.35	-17.96	0.699	0.014	25.7			27.3	14.4	23.9			
HC_CC_A1	HC-CC-A	1		-5.30	-17.89	0.689	0.009	28.3			30.9	16.7	28.2			
HC_CC_B1		1		-4.31	-17.66	0.686	0.011	29.1			31.9	17.4	29.5			
HC_CC_B2	HC-CC-B	1		-4.36	-17.74	0.694	0.009	26.9			28.9	15.4	25.8			
HC_CC_C1		1		-5.40	-16.70	0.720	0.008	20.8			20.5	10.0	15.8			
HC_CC_C2	HC-CC-C	1		-5.50	-16.79	0.669	0.010	33.2			37.7	20.9	36.6			
HC_CC_D1		1		-4.40	-16.97	0.695	0.014	26.8			28.7	15.3	25.6			
HC_CC_D2	HC-CC-D	1		-4.51	-17.49	0.709	0.010	23.4			24.1	12.4	20.1			
<b>Site P means:</b>				<b>-66</b>	<b>-4.89</b>	<b>-17.40</b>	<b>0.695</b>	<b>0.002</b>	<b>26.7</b>	<b>1.5</b>	<b>1.2</b>	<b>-15.5</b>	<b>0.3</b>	<b>28.8</b>	<b>15.3</b>	<b>25.7</b>
HC_GG_A1	HC-GG-A	1		0.98	-12.25	0.652	0.009	37.9			44.5	25.1	45.0			
HC_GG_B1	HC-GG-B	1		-5.61	-11.83	0.701	0.012	25.3			26.7	14.0	23.1			
HC_GG_C1	HC-GG-C	1		-2.36	-9.83	0.684	0.009	29.5			32.5	17.7	30.3			
<b>Site O (gastropod) means:</b>				-20.5	<b>-2.33</b>	<b>-11.31</b>	<b>0.679</b>	<b>0.014</b>	<b>30.8</b>	<b>7.5</b>	<b>7.3</b>	<b>-8.6</b>	<b>0.8</b>	<b>34.6</b>	<b>18.9</b>	<b>32.8</b>
HC_HB1_A1		1		-6.00	-9.90	0.711	0.009	23.0			23.5	12.0	19.4			
HC_HB1_A2	HC-HB1-A	1		-6.00	-9.90	0.711	0.009	22.9			23.4	11.9	19.3			
HC_HB1_C_1		2		-5.76	-9.89	0.723	0.016	20.1			19.6	9.4	14.7			
HC_HB1_C1	HC-HB1-C	1		-5.68	-9.94	0.715	0.008	21.9			22.0	11.0	17.6			
<b>Site T (bivalve) means:</b>				<b>-5.86</b>	<b>-9.91</b>	<b>0.715</b>	<b>0.003</b>	<b>22.0</b>	<b>2.0</b>	<b>1.6</b>	<b>-8.9</b>	<b>0.4</b>	<b>22.1</b>	<b>11.1</b>	<b>17.7</b>	
HC_HB1_G1	HC-HB1-G	1		-8.14	-13.51	0.685	0.008	<b>29.1</b>			32.0	17.4	29.6			
HC_HB1_H1	HC-HB1-H	1		-6.67	-13.09	0.677	0.011	<b>31.2</b>			34.9	19.2	33.1			
<b>Site T (gastropod) means:</b>				54	<b>-7.40</b>	<b>-13.30</b>	<b>0.681</b>	<b>0.004</b>	<b>30.1</b>	<b>2.0</b>	<b>2.0</b>	<b>-10.7</b>	<b>0.4</b>	<b>33.4</b>	<b>18.3</b>	<b>31.3</b>
HC_HD_A1		1		-6.88	-8.78	0.673	0.011	32.2			36.3	20.1	34.8			
HC_HD_A2		1		-6.85	-8.72	0.699	0.010	25.8			27.3	14.4	23.9			
HC_HD_A3	HC-HD-A	1		-6.79	-8.65	0.681	0.010	30.2			33.5	18.3	31.4			
HC_HD_B_1		2		-5.83	-11.98	0.716	0.010	21.9			21.9	11.0	17.5			
HC_HD_B1	HC-HD-B	1		-5.93	-11.84	0.682	0.010	30.0			33.2	18.2	31.1			
HC_HD_D1		1		-6.56	-8.43	0.701	0.008	25.3			26.7	14.0	23.2			
HC_HD_D2	HC-HD-D	1		-6.55	-8.45	0.723	0.008	20.3			19.8	9.6	14.9			

	Site M means:		-66	<b>-6.43</b>	<b>-9.69</b>	<b>0.698</b>	<b>0.008</b>	<b>25.9</b>	<b>4.0</b>	<b>3.7</b>	<b>-7.9</b>	<b>0.6</b>	<b>27.7</b>	<b>14.7</b>	<b>24.5</b>
HC_L5233A_A1		1		-4.12	-8.71	0.694	0.011	27.0					29.0	15.5	26.0
HC_L5233A_A2	HC-L5233A-A	1		-4.01	-8.67	0.697	0.008	26.4					28.2	15.0	25.0
HC_L5233A_B1		1		-5.65	-8.54	0.695	0.010	26.8					28.7	15.3	25.6
HC_L5233A_B2	HC-L5233A-B	1		-5.81	-8.70	0.659	0.009	35.8					41.5	23.3	41.3
HC_L5233A_D_1		2		-5.22	-9.52	0.645	0.012	39.8					47.3	26.8	48.5
HC_L5233A_D_2		2		-5.25	-9.49	0.662	0.011	35.2					40.6	22.7	40.2
HC_L5233A_D1	HC-L5233A-D	1		-5.26	-9.52	0.696	0.009	26.5					28.3	15.1	25.1
Site K means:		-26		<b>-5.01</b>	<b>-8.94</b>	<b>0.680</b>	<b>0.007</b>	<b>30.5</b>	<b>3.5</b>	<b>3.5</b>	<b>-6.3</b>	<b>0.5</b>	<b>34.1</b>	<b>18.7</b>	<b>32.3</b>
HC_MCD_A1		1		-5.67	-10.54	0.686	0.009	29.0					31.8	17.2	29.3
HC_MCD_A2	HC-MCD-A	1		-5.73	-10.55	0.694	0.011	27.0					29.0	15.5	26.0
HC_MCD_B_1		2		-4.59	-10.48	0.701	0.011	25.4					26.8	14.1	23.3
HC_MCD_B1	HC-MCD-B	1		-4.68	-10.61	0.688	0.009	28.6					31.2	16.9	28.6
HC_MCD_D_1		2		-4.32	-10.79	0.657	0.010	36.4					42.4	23.8	42.4
HC_MCD_D_2		2		-4.34	-10.91	0.685	0.015	29.2					32.1	17.5	29.7
HC_MCD_D2	HC-MCD-D	1		-4.65	-10.53	0.703	0.009	24.9					26.1	13.7	22.5
Site H means:		34		<b>-4.92</b>	<b>-10.61</b>	<b>0.689</b>	<b>0.004</b>	<b>28.3</b>	<b>2.0</b>	<b>1.9</b>	<b>-8.4</b>	<b>0.4</b>	<b>31.0</b>	<b>16.7</b>	<b>28.4</b>
HC_ST_B1		1		-7.09	-9.43	0.673	0.010	32.2					36.4	20.1	34.9
HC_ST_B2	HC-ST-B	1		-7.13	-9.36	0.688	0.010	28.5					31.1	16.8	28.4
HC_ST_D1		1		-6.88	-9.59	0.694	0.010	27.0					29.1	15.5	26.0
HC_ST_D2	HC-ST-D	1		-6.90	-9.62	0.666	0.011	34.1					39.1	21.8	38.3
Site R means:		-25		<b>-7.00</b>	<b>-9.50</b>	<b>0.680</b>	<b>0.000</b>	<b>30.4</b>	<b>1.5</b>	<b>0.2</b>	<b>-6.8</b>	<b>0.7</b>	<b>33.9</b>	<b>18.6</b>	<b>31.9</b>
HC_Vein	Vein	1		<b>-10.06</b>	<b>-14.965</b>	<b>0.622</b>	<b>0.006</b>	<b>46.1</b>	<b>4.0</b>		<b>-8.6</b>	<b>0.5</b>	<b>56.7</b>	<b>32.3</b>	<b>60.4</b>
			<b>-15</b>												
S12078_1		2		-7.03	-9.03	0.686	0.008	28.9					31.7	17.2	29.2
S12078_2		2		-7.17	-8.76	0.732	0.010	18.2					17.0	7.7	11.6
S12078_3	S12078	2		-7.12	-8.78	0.693	0.009	27.2					29.3	15.7	26.4
S12079_1		2		-6.46	-10.73	0.712	0.018	22.8					23.3	11.8	19.1
S12079_2	S12079	2		-6.46	-10.87	0.677	0.013	31.2					35.0	19.3	33.2
S12080_1		2		-6.94	-8.67	0.675	0.012	31.7					35.6	19.6	34.0
S12080_3		2		-7.00	-8.75	0.759	0.011	12.3					9.1	2.5	2.5
S12080_4	S12080	2		-6.92	-8.56	0.688	0.011	28.5					31.1	16.9	28.6
Site G means:		-10.7		<b>-6.84</b>	<b>-9.44</b>	<b>0.702</b>	<b>0.004</b>	<b>25.1</b>	<b>2.0</b>	<b>1.7</b>	<b>-7.8</b>	<b>0.4</b>	<b>26.8</b>	<b>14.0</b>	<b>23.4</b>
S12082_1		2		-3.08	-19.82	0.710	0.012	23.2					23.8	12.1	19.7
S12082_2		2		-3.17	-19.60	0.766	0.011	10.9					7.2	1.2	0.3
S12082_3	S12082	2		-3.08	-19.78	0.654	0.017	37.2					43.5	24.5	43.7
S12083_2		2		-4.72	-19.92	0.731	0.011	18.3					17.1	7.8	11.7
S12083_3	S12083	2		-4.65	-19.84	0.676	0.009	31.4					35.2	19.4	33.5
S12085_1		2		-3.35	-20.29	0.702	0.015	25.1					26.3	13.8	22.7

S12085_2		2	-3.44	-20.02	0.736	0.009	17.2					15.6	6.8	10.0
S12085_3	S12085	2	-3.35	-20.18	0.719	0.007	21.0					20.8	10.2	16.1
	<b>Site L (L6214) means:</b>	-4.3	<b>-3.73</b>	<b>-19.92</b>	<b>0.711</b>	<b>0.004</b>	<b>22.9</b>	<b>2.0</b>	<b>2.2</b>	<b>-18.8</b>	<b>0.4</b>	<b>24.0</b>	<b>12.2</b>	<b>20.0</b>
S12086_1		2	-5.46	-17.60	0.709	0.007	23.3					24.0	12.3	19.9
S12086_2	S12086	2	-5.82	-14.93	0.679	0.007	30.7					34.2	18.8	32.3
S12087_1		2	-5.23	-17.05	0.702	0.012	25.1					26.4	13.8	22.8
S12087_2	S12087	2	-5.40	-16.90	0.752	0.007	13.9					11.2	3.9	4.9
S12089_1		2	-3.81	-19.82	0.723	0.007	20.1					19.6	9.4	14.7
S12089_2	S12089	2	-3.82	-19.45	0.713	0.015	22.4					22.7	11.4	18.3
S12090_1		2	-4.74	-17.19	0.731	0.013	18.5					17.4	8.0	12.1
S12090_2	S12090	2	-4.73	-17.08	0.690	0.009	28.1					30.6	16.5	27.8
	<b>Site L (L6215) means:</b>	-1.5	<b>-4.88</b>	<b>-17.50</b>	<b>0.712</b>	<b>0.007</b>	<b>22.6</b>	<b>3.5</b>	<b>3.2</b>	<b>-16.4</b>	<b>0.4</b>	<b>23.2</b>	<b>11.8</b>	<b>19.1</b>
S13114_1		2	-5.60	-17.30	0.732	0.009	18.2					17.0	7.7	11.7
S13114_2	S13114	2	-5.52	-17.31	0.675	0.007	31.8					35.7	19.7	34.1
S13115_1		2	-5.35	-16.56	0.683	0.015	29.7					32.8	17.9	30.6
S13115_2	S13115	2	-5.34	-16.73	0.711	0.008	22.9					23.3	11.9	19.2
S13116_1		2	-5.20	-18.55	0.732	0.008	18.3					17.1	7.8	11.7
S13116_2	S13116	2	-5.27	-18.70	0.699	0.010	25.8					27.4	14.5	24.0
	<b>Site X means:</b>	35	<b>-5.38</b>	<b>-17.52</b>	<b>0.705</b>	<b>0.005</b>	<b>24.3</b>	<b>2.5</b>	<b>2.5</b>	<b>-16.1</b>	<b>0.4</b>	<b>25.6</b>	<b>13.2</b>	<b>21.9</b>

	This study	Dennis2013												
Mean of all fossil shells:	0.699	0.683										0.604	0.685	
st.dev:	0.014	0.003										0.576	0.657	
n:	33.000	4.000										0.633	0.714	

#### Bold columns used to generate data for figure

Key to column headings:

Analysis - Unique isotopic analysis name assigned during measurement of sample

Sample - A single fossil specimen

Batch - Whether the sample was run as part of 2010 (Batch 1) or 2012 (Batch 2) set of analyses

Strat - Stratigraphic height relative to the K-Pg boundary

d13c, d18o - isotopic values for carbon and oxygen respectively

ARF D47 - Delta47 converted to the Absolute Reference Frame c

se - standard error on D47 analysis

T(zaarur) - temperature calculated using Zaarur 2013 calibration absolute reference fram equation

95% Conf (from Graph) - reading off the expected 95% confidence interval from Zaarur Fig. 2b

95% Conf (samp) - Standard error calculated from average of different sample temperatures, multiplied by 1.96 to get 95% confidence (altman2005)

d18ow - Reconstructed d18O of water

d18ow 1sd = 1 stdev error on d18ow

Eagle2013 (2) - Temperature reconstructed from D47 using 2 different calibrations from Eagle 2013 study

Henkes2013 - Temperature reconstructed using calibration from Henkes 2013 study

Data used to generate Figure 2 are the Bold rows above, and are simplified below

Sample	Batch	Strat	d13C	d18O	ARF D47	se	T(Zaarur)	95%(from Gr)	95%sample(S)	d18Ow	d18Ow err	Eagle2013Ara	Eagle2013Bio	Henkes2013T
Lousiana (Modern) Mean:	0	-8.63	-5.19	0.695	0.005	26.7	2.5	2.6	-3.2	0.4	28.8	15.3	25.7	
Site P means:	-66	-4.89	-17.40	0.695	0.002	26.7	1.5	1.2	-15.5	0.3	28.8	15.3	25.7	
Site O (gastropod) means:	-20.5	-2.33	-11.31	0.679	0.014	30.8	7.5	7.3	-8.6	0.8	34.6	18.9	32.8	
Site T (bivalve) means:	0	-5.86	-9.91	0.715	0.003	22.0	2	1.6	-8.9	0.4	22.1	11.1	17.7	
Site T (gastropod) means:	54	-7.40	-13.30	0.681	0.004	30.1	2	2.0	-10.7	0.4	33.4	18.3	31.3	
Site M means:	-66	-6.43	-9.69	0.698	0.008	25.9	4	3.7	-7.9	0.6	27.7	14.7	24.5	
Site K means:	-26	-5.01	-8.94	0.680	0.007	30.5	3.5	3.5	-6.3	0.5	34.1	18.7	32.3	
Site H means:	34	-4.92	-10.61	0.689	0.004	28.3	2	1.9	-8.4	0.4	31.0	16.7	28.4	
Site R means:	-25	-7.00	-9.50	0.680	0.000	30.4	1.5	0.2	-6.8	0.7	33.9	18.6	31.9	
Vein	-15	-10.06	-14.96	0.622	0.006	46.1	4	0.0	-8.6	0.5	56.7	32.3	60.4	
Site G means:	-10.7	-6.84	-9.44	0.702	0.004	25.1	2	1.7	-7.8	0.4	26.8	14.0	23.4	
Site L (L6214) means:	-4.3	-3.73	-19.92	0.711	0.004	22.9	2	2.2	-18.8	0.4	24.0	12.2	20.0	
Site L (L6215) means:	-1.5	-4.88	-17.50	0.712	0.007	22.6	3.5	3.2	-16.4	0.4	23.2	11.8	19.1	
Site X means:	35	-5.38	-17.52	0.705	0.005	24.3	2.5	2.5	-16.1	0.4	25.6	13.2	21.9	

Table DR3. Raw Clumped Data

Sample ID	voltage (mV)	$\delta^{13}\text{C}$ (PDB)	$\delta^{13}\text{C}$ stdev	$\delta^{18}\text{O}$ gas (SMOW)	$\delta^{18}\text{O}$ mineral (PDB)	$\delta^{18}\text{O}$ stdev	$\delta_{47}$ (v. Oz)	$\delta_{47}$ stdev	$\Delta_{47}$ (v. Oz)	$\Delta_{47}$ stdev	$\Delta_{47}$ sterror	$\delta_{48}$ (v. Oz)	$\delta_{48}$ stdev	$\Delta_{48}$ (v. Oz)	$\Delta_{48}$ stdev	slope	int	HG corr	stretch	acid	Accepted D47	Res. Eq5	Res. Eq6	ARF D47
Samples (Includes samples that were culled from final data set for D48 and contamination issues)																								
512078	15677	-7.167	0.009	30.224	-8.755	0.015	1.465	0.021	-0.253	0.029	0.010	11.978	1.807	0.317	0.004	-0.859	0.599	0.589	0.669		-0.260	0.651	0.732	
512078	15761	-7.116	0.008	30.194	-8.784	0.012	1.447	0.023	-0.291	0.026	0.009	12.107	1.993	0.409	0.004	-0.859	0.562	0.553	0.633		-0.297	0.612	0.693	
512078	15808	-7.031	0.004	29.937	-9.032	0.004	1.268	0.029	-0.298	0.024	0.008	11.724	2.114	0.399	0.004	-0.859	0.555	0.546	0.626		-0.303	0.605	0.686	
512079	15748	-6.459	0.011	28.171	-10.731	0.016	0.902	0.023	-0.279	0.050	0.018	7.407	1.261	0.335	0.004	-0.859	0.579	0.570	0.650		-0.279	0.631	0.712	
512079	15771	-6.456	0.010	28.029	-10.867	0.012	-0.080	0.021	-0.313	0.036	0.013	7.213	1.345	0.229	0.004	-0.859	0.546	0.538	0.618		-0.312	0.596	0.677	
512080	15808	-6.938	0.009	30.314	-8.669	0.015	1.724	0.025	-0.307	0.034	0.012	12.693	2.338	0.390	0.004	-0.859	0.544	0.536	0.616		-0.314	0.594	0.675	
512080	15726	-6.934	0.008	30.625	-8.369	0.016	1.974	0.028	-0.367	0.032	0.011	13.779	2.810	0.288	0.004	-0.859	0.483	0.475	0.555		-0.376	0.530	0.611	
512080	14837	-7.005	0.022	30.225	-8.754	0.026	1.651	0.020	-0.227	0.030	0.011	12.246	2.069	0.384	0.004	-0.859	0.625	0.615	0.695		-0.234	0.678	0.759	
512080	15877	-6.920	0.009	30.430	-8.557	0.010	1.869	0.019	-0.294	0.030	0.011	13.142	2.556	0.218	0.004	-0.859	0.556	0.548	0.628		-0.302	0.607	0.688	
512082	15796	-3.079	0.010	18.727	-19.817	0.012	-6.051	0.015	-0.306	0.034	0.012	-15.417	-3.230	0.423	0.004	-0.859	0.578	0.570	0.650		-0.281	0.629	0.710	
512082	15689	-3.170	0.014	18.955	-19.598	0.023	-5.858	0.019	-0.252	0.032	0.011	-15.121	-3.376	0.404	0.004	-0.859	0.632	0.622	0.702		-0.227	0.685	0.766	
512082	15817	-3.079	0.013	18.765	-19.781	0.020	-6.066	0.019	-0.360	0.049	0.017	-14.982	-2.864	0.435	0.004	-0.859	0.525	0.517	0.597		-0.334	0.573	0.654	
512083	15745	-4.750	0.007	19.542	-19.033	0.044	-7.408	0.019	-0.872	0.044	0.016	-6.807	3.889	0.347	0.004	-0.859	0.019	0.019	0.099		-0.840	0.046	0.127	
512083	15705	-4.715	0.012	18.617	-19.923	0.016	-7.717	0.019	-0.293	0.030	0.011	-16.028	-3.628	0.463	0.004	-0.859	0.599	0.590	0.670		-0.260	0.650	0.731	
512083	15810	-4.652	0.009	18.708	-19.836	0.015	-7.619	0.024	-0.345	0.024	0.009	-15.393	-3.161	0.263	0.004	-0.859	0.546	0.538	0.618		-0.313	0.595	0.676	
512085	15859	-3.352	0.003	18.238	-20.288	0.009	-6.809	0.010	-0.317	0.042	0.015	-16.502	-3.372	0.190	0.004	-0.859	0.571	0.562	0.642		-0.288	0.621	0.702	
512085	15835	-3.442	0.006	18.519	-20.017	0.009	-6.583	0.027	-0.283	0.025	0.009	-16.060	-3.474	0.288	0.004	-0.859	0.604	0.595	0.675		-0.255	0.655	0.736	
512085	15795	-3.354	0.006	18.355	-20.175	0.012	-6.678	0.022	-0.300	0.019	0.007	-16.419	-3.517	0.349	0.004	-0.859	0.588	0.578	0.658		-0.272	0.638	0.719	
512086	15862	-5.465	0.007	21.034	-17.597	0.008	-6.053	0.028	-0.307	0.020	0.007	-9.867	-2.122	0.164	0.004	-0.859	0.578	0.569	0.649		-0.281	0.628	0.709	
512086	15964	-5.816	0.010	23.808	-14.928	0.015	-3.659	0.019	-0.326	0.020	0.007	-2.976	-0.607	0.247	0.004	-0.859	0.548	0.540	0.620		-0.310	0.598	0.679	
512087	15868	-5.232	0.010	21.603	-17.050	0.015	-5.269	0.025	-0.311	0.035	0.012	-8.384	-1.739	0.263	0.004	-0.859	0.571	0.562	0.642		-0.288	0.621	0.702	
512087	15718	-5.396	0.009	21.759	-16.899	0.012	-5.223	0.014	-0.263	0.019	0.007	-8.406	-2.066	0.209	0.004	-0.859	0.618	0.609	0.689		-0.241	0.671	0.752	
512089	15859	-3.811	0.007	18.724	-19.820	0.011	-6.746	0.028	-0.297	0.020	0.007	-15.519	-3.325	0.234	0.004	-0.859	0.591	0.582	0.662		-0.268	0.642	0.723	
512089	15675	-3.824	0.009	19.112	-19.447	0.015	-6.381	0.028	-0.304	0.042	0.015	-14.579	-3.132	0.317	0.004	-0.859	0.582	0.573	0.653		-0.277	0.632	0.713	
512090	15841	-4.737	0.007	21.459	-17.188	0.011	-4.906	0.024	-0.282	0.037	0.013	-8.937	-2.018	0.210	0.004	-0.859	0.598	0.589	0.669		-0.261	0.650	0.731	
512090	15829	-4.732	0.007	21.574	-17.078	0.014	-4.826	0.019	-0.321	0.024	0.009	-8.340	-1.640	0.265	0.004	-0.859	0.559	0.550	0.630		-0.300	0.609	0.690	
513114	15807	-5.597	0.008	21.343	-17.301	0.010	-5.853	0.022	-0.285	0.025	0.009	-9.212	-2.064	0.202	0.004	-0.859	0.599	0.590	0.670		-0.260	0.651	0.732	
513114	15825	-5.516	0.006	21.331	-1																			

TV01	15874	2.332	0.010	30.446	-8.542	0.015	10.923	0.029	-0.242	0.018	0.006	13.116	2.460	0.326	0.004	-0.859	0.570	0.561	0.641	0.662
CHM1	15663	2.252	0.013	37.323	-1.924	0.035	17.330	0.017	-0.626	0.045	0.016	30.956	6.645	0.402	0.004	-0.859	0.159	0.156	0.236	0.352
TV01	15725	2.369	0.010	30.276	-8.706	0.014	10.794	0.019	-0.236	0.030	0.011	12.633	2.313	0.208	0.004	-0.859	0.577	0.567	0.647	0.662
CHM1	15767	2.268	0.010	37.151	-2.090	0.015	17.353	0.008	-0.450	0.034	0.012	29.214	5.278	0.281	0.004	-0.859	0.335	0.330	0.410	0.352
TV01	15844	2.439	0.011	30.292	-8.690	0.015	10.922	0.017	-0.194	0.026	0.009	12.690	2.337	0.428	0.004	-0.859	0.618	0.609	0.689	0.662
CHM1	15865	2.317	0.010	37.262	-1.983	0.012	17.463	0.025	-0.498	0.033	0.012	29.902	5.734	0.188	0.004	-0.859	0.287	0.282	0.362	0.352
TV01	15838	2.385	0.007	30.329	-8.654	0.012	10.882	0.013	-0.218	0.037	0.013	12.988	2.560	0.287	0.004	-0.859	0.595	0.586	0.666	0.662
CHM1	15870	2.294	0.010	37.224	-2.020	0.012	17.415	0.016	-0.486	0.024	0.008	29.678	5.588	0.296	0.004	-0.859	0.298	0.294	0.374	0.352

#### Heated and Equilibrated Gases

BOC	15870	-10.767	0.008	28.720	-10.202	0.013	-4.108	0.027	-0.848	0.032	0.011	8.569	1.365	0.370					
eBOC	15810	-10.690	0.004	57.182	17.183	0.007	24.204	0.021	-0.710	0.031	0.011	78.767	14.226	0.167	Values for Converting to ARF (see Dennis et al. 2011)				
BOC	15914	-10.730	0.002	29.306	-9.639	0.006	-3.534	0.016	-0.887	0.039	0.014	10.005	1.652	0.212					
eBOC	15816	-10.985	0.010	59.235	19.159	0.014	25.878	0.035	-0.769	0.031	0.011	83.920	15.129	0.340	HG Slope=	0.00425			
BOC	15769	-10.542	0.008	28.649	-10.270	0.012	-3.986	0.019	-0.874	0.025	0.009	8.064	1.001	0.278	HG Intercep	-0.85888			
eBOC	15820	-10.938	0.005	60.193	20.080	0.008	26.886	0.027	-0.753	0.032	0.011	86.380	15.597	0.163					
BOC	15919	-10.789	0.012	29.589	-9.366	0.017	-3.335	0.025	-0.911	0.033	0.012	10.675	1.766	0.316	Equil Intercep	0.00362			
eBOC	15986	-11.050	0.011	60.091	19.982	0.015	26.681	0.023	-0.746	0.035	0.013	86.363	15.776	0.301					
BOC	15979	-10.602	0.007	59.687	19.593	0.012	26.720	0.020	-0.755	0.036	0.013	85.579	15.816	0.336	ETF Coeffic	1.042			
eBOC	16014	-10.857	0.004	59.934	19.830	0.006	26.715	0.015	-0.749	0.021	0.007	86.298	16.017	0.240		0.921			
BOC	15886	-10.750	0.008	28.807	-10.118	0.013	-4.018	0.024	-0.860	0.025	0.009	8.784	1.411	0.417					
eBOC	15913	-11.065	0.011	59.805	19.707	0.016	26.401	0.019	-0.729	0.017	0.006	85.898	15.890	0.286					
std gas	15579	-9.277	0.007	64.102	23.841	0.010	33.359	0.022	0.164	0.035	0.012	95.731	16.827	0.261					
Eq Gas	15916	-7.995	2.264	32.361	-6.699	1.287	3.020	0.022	-0.013	0.178	0.063	17.855	3.462	0.838					
HG	15879	-9.250	0.006	64.299	24.031	0.010	33.579	0.021	0.162	0.030	0.011	97.042	17.667	0.308					
equil gas	16025	-10.424	0.008	31.963	-7.082	0.016	0.306	0.023	0.034	0.039	0.014	17.142	3.545	0.293					
equil gas	15952	-10.783	0.005	61.225	21.073	0.009	28.975	0.031	0.136	0.037	0.013	89.894	16.902	0.258					
equil gas	15942	-10.630	0.006	31.550	-7.480	0.006	-0.334	0.017	0.002	0.035	0.013	15.750	2.975	0.368					

Sample	d13C (PDB)	d13C stdev	d18O gas (SMOW)	d18O mined (PDB)	d18O stdev	d47 (v. Oz)	d47 stdev	D47 (v. Oz)	D47 stdev	D47 sterror	d48 (v. Oz)	D48 (v. Oz)	D48 stdev	D47's			
<b>Samples (includes samples later culled for D48 and contamination reasons)</b>																HG Corr.	Stretch Co Acid Corr.
HC-CC-A	-5.301	0.006	20.725	-17.895	0.009	-6.221	0.020	-0.365	0.044	0.016	-11.357	-3.078	0.277	0.526	0.549	0.629	
HC-CC-B	-4.314	0.005	20.972	-17.657	0.013	-5.013	0.028	-0.352	0.035	0.012	-10.899	-3.104	0.588	0.523	0.546	0.626	
HC-CC-B	-4.355	0.005	20.886	-17.740	0.004	-5.132	0.014	-0.345	0.022	0.008	-11.065	-3.103	0.457	0.531	0.554	0.634	
HC-CC-C	-5.400	0.007	21.970	-16.697	0.006	-5.037	0.011	-0.320	0.030	0.011	-8.570	-2.701	0.582	0.555	0.579	0.659	
HC-CC-C	-5.501	0.005	21.870	-16.793	0.008	-5.282	0.023	-0.370	0.043	0.015	-8.631	-2.567	0.646	0.508	0.531	0.611	
HC-CC-D	-4.510	0.008	21.144	-17.492	0.008	-5.010	0.017	-0.330	0.027	0.010	-9.923	-2.455	0.541	0.545	0.568	0.648	
HC-GG-A	0.985	0.006	29.544	-9.410	0.012	8.802	0.028	-0.194	0.028	0.010	11.765	2.824	0.384	0.502	0.524	0.604	
HC-GG-B	-5.606	0.005	29.978	-8.992	0.009	2.787	0.050	-0.243	0.029	0.010	12.926	3.157	0.421	0.530	0.554	0.634	
HC-GG-C	-2.362	0.006	29.103	-9.833	0.005	5.089	0.017	-0.221	0.034	0.012	10.581	2.522	0.475	0.523	0.546	0.626	
HC-HB1-I	-6.004	0.009	29.032	-9.902	0.018	1.462	0.018	-0.243	0.012	0.004	10.443	2.539	0.576	0.548	0.572	0.652	
HC-HB1-C	-5.682	0.007	28.988	-9.944	0.011	1.739	0.013	-0.236	0.023	0.008	9.886	2.071	0.337	0.552	0.576	0.656	
HC-HB1-I	-5.224	0.006	29.550	-9.404	0.006	2.741	0.018	-0.235	0.036	0.013	11.926	2.999	0.556	0.539	0.563	0.643	
HC-HB1-C	-8.142	0.007	28.230	-10.674	0.016	-1.471	0.024	-0.309	0.013	0.005	8.643	2.323	0.433	0.520	0.543	0.623	
HC-HC-D	-6.559	0.005	30.563	-8.429	0.009	2.445	0.014	-0.240	0.031	0.011	14.645	3.725	0.539	0.539	0.562	0.642	
HC-HD-A	-6.880	0.005	30.200	-8.778	0.005	1.739	0.015	-0.274	0.042	0.015	14.369	4.160	0.494	0.513	0.535	0.615	
HC-HD-A	-6.847	0.006	30.258	-8.723	0.010	1.853	0.015	-0.249	0.042	0.015	13.935	3.618	0.486	0.537	0.560	0.640	
HC-HD-A	-6.794	0.007	30.337	-8.646	0.016	1.968	0.022	-0.264	0.033	0.012	14.265	3.789	0.478	0.520	0.543	0.623	
HC-HD-B	-5.934	0.008	27.017	-11.841	0.007	-0.522	0.014	-0.296	0.031	0.011	4.852	0.904	0.700	0.521	0.543	0.623	
HC-HD-D	-6.553	0.008	30.539	-8.452	0.013	2.447	0.010	-0.220	0.028	0.010	14.662	3.789	0.619	0.558	0.583	0.663	
HC-L523C	-4.119	0.006	30.267	-8.714	0.007	4.542	0.017	-0.219	0.043	0.015	13.853	3.508	0.588	0.532	0.556	0.636	
HC-L523C	-4.014	0.008	30.312	-8.670	0.004	4.694	0.015	-0.214	0.030	0.011	13.730	3.296	0.701	0.535	0.558	0.638	
HC-L523C	-5.652	0.008	30.450	-8.538	0.008	3.218	0.007	-0.235	0.044	0.015	14.169	3.471	0.724	0.533	0.556	0.636	
HC-L523C	-5.264	0.007	29.427	-9.522	0.006	2.573	0.026	-0.242	0.018	0.006	11.799	3.112	0.420	0.534	0.557	0.637	
HC-MCD-	-5.673	0.006	28.372	-10.537	0.012	1.101	0.016	-0.271	0.025	0.009	8.676	2.069	0.520	0.525	0.548	0.628	
HC-MCD-	<b>-5.729</b>	<b>0.004</b>	<b>28.353</b>	<b>-10.555</b>	<b>0.010</b>	<b>1.034</b>	<b>0.019</b>	<b>-0.264</b>	<b>0.050</b>	<b>0.018</b>	<b>9.891</b>	<b>3.312</b>	<b>1.280</b>	<b>0.532</b>	<b>0.555</b>	<b>0.635</b>	
HC-MCD-	-4.680	0.006	28.295	-10.611	0.006	2.000	0.023	-0.258	0.037	0.013	8.760	2.297	0.526	0.526	0.549	0.629	
HC-MCD-	<b>-4.299</b>	<b>0.006</b>	<b>28.113</b>	<b>-10.786</b>	<b>0.009</b>	<b>3.603</b>	<b>0.014</b>	<b>1.154</b>	<b>0.044</b>	<b>0.016</b>	<b>8.675</b>	<b>2.566</b>	<b>0.502</b>	<b>1.917</b>	<b>2.001</b>	<b>2.081</b>	
HC-MCD-	-4.653	0.004	28.378	-10.531	0.006	2.124	0.016	-0.242	0.028	0.010	8.916	2.290	0.452	0.540	0.564	0.644	
HC-ST-A	<b>-6.990</b>	<b>0.005</b>	<b>29.716</b>	<b>-9.244</b>	<b>0.006</b>	<b>12.308</b>	<b>0.027</b>	<b>10.866</b>	<b>0.035</b>	<b>0.012</b>	<b>15.984</b>	<b>6.705</b>	<b>0.241</b>	<b>11.516</b>	<b>12.020</b>	<b>12.100</b>	
HC-ST-B	-7.092	0.008	29.524	-9.428	0.004	0.851	0.015	-0.286	0.014	0.005	11.574	2.708	0.629	0.513	0.535	0.615	
HC-ST-B	-7.127	0.007	29.598	-9.358	0.004	0.905	0.021	-0.272	0.041	0.014	11.843	2.832	0.560	0.526	0.549	0.629	
HC-ST-D	-6.878	0.006	29.353	-9.593	0.006	0.909	0.016	-0.266	0.020	0.007	11.457	2.924	0.648	0.532	0.555	0.635	
HC-ST-D	-6.900	0.005	29.322	-9.623	0.004	0.830	0.026	-0.293	0.044	0.015	11.276	2.806	0.744	0.506	0.528	0.608	
HC-VEIN	-10.065	0.007	23.436	-15.286	0.006	-8.197	0.016	-0.436	0.016	0.006	-4.005	-0.954	0.439	0.481	0.502	0.582	
<b>Heated Gases</b>																HG Slope=	0.013
BOC	-10.827	0.005	29.738	-9.222	0.028	-3.121	0.030	-0.846	0.033	0.012	11.920	2.651	0.176				
BOC	-11.189	0.007	28.036	-10.860	0.002	-5.163	0.008	-0.858	0.031	0.011	7.484	1.562	0.386	HG Intercept= -0.810			
BOC	-11.020	0.008	28.901	-10.029	0.017	-4.149	0.021	-0.861	0.046	0.016	9.881	2.260	0.406				
HEATED C	-11.017	0.008	58.306	18.264	0.018	25.266	0.014	-0.479	0.029	0.010	87.915	20.599	0.321				
BOC	-10.369	0.003	30.530	-8.461	0.098	-1.895	0.015	-0.846	0.038	0.013	14.417	3.582	0.411				
Heated E	<b>-10.730</b>	<b>0.008</b>	<b>59.116</b>	<b>19.044</b>	<b>0.015</b>	<b>26.349</b>	<b>0.008</b>	<b>-0.483</b>	<b>0.028</b>	<b>0.010</b>	<b>91.844</b>	<b>22.719</b>	<b>0.381</b>				
Heated G	-10.690	0.009	29.385	-9.563	0.010	-3.342	0.015	-0.852	0.032	0.011	11.496	2.918	0.522				
Heated G	-10.749	0.009	29.833	-9.131	0.003	-2.962	0.021	-0.856	0.034	0.012	12.173	2.717	0.180				
Heated G	-10.777	0.010	59.535	19.447	0.015	26.729	0.020	-0.470	0.038	0.013	93.133	23.118	0.516				

Heated G	-10.748	0.008	29.742	-9.218	0.041	-3.045	0.018	-0.850	0.031	0.011	12.178	2.899	0.450
Heated G	-10.799	0.009	59.275	19.197	0.016	26.452	0.015	-0.468	0.016	0.006	91.856	22.422	0.506
Heated G	-10.779	0.009	58.416	18.370	0.009	25.636	0.017	-0.455	0.037	0.013	90.224	22.551	0.537
Heated G	-10.793	0.010	28.978	-9.954	0.009	-3.842	0.028	-0.850	0.045	0.016	10.425	2.649	0.490
Heated BO	-10.755	0.011	30.172	-8.805	0.009	-2.640	0.016	-0.864	0.036	0.013	13.797	3.665	0.628

## Standards

Accepted value (Dennis et al. 2

CHM1	2.301	0.006	37.395	-1.856	0.006	17.816	0.022	-0.306	0.036	0.013	33.244	8.682	0.537	0.273	0.285	0.365	0.392
CHM1	2.325	0.006	37.428	-1.823	0.008	17.848	0.024	-0.330	0.044	0.016	32.844	8.225	0.619	0.2476	0.258	0.338	0.392
CHM1	2.257	0.007	37.335	-1.913	0.010	17.696	0.018	-0.323	0.031	0.011	31.878	7.464	0.462	0.2572	0.268	0.348	0.392
CHM1	2.310	0.003	37.383	-1.867	0.005	17.791	0.023	-0.330	0.029	0.010	32.136	7.621	0.320	0.2484	0.259	0.339	0.392
CHM1	2.328	0.006	37.403	-1.848	0.014	17.841	0.016	-0.315	0.018	0.006	32.901	8.331	0.651	0.2629	0.274	0.354	0.392
CHM1	2.319	0.006	37.368	-1.882	0.003	17.850	0.012	-0.263	0.026	0.009	32.377	7.887	0.359	0.3153	0.329	0.409	0.392
CHM1	2.333	0.006	37.367	-1.882	0.006	17.808	0.031	-0.317	0.046	0.016	32.758	8.260	0.461	0.261	0.273	0.353	0.392
CORAL 4E	0.168	0.009	43.038	3.574	0.009	21.767	0.011	0.092	0.022	0.008	48.033	12.100	0.431	0.6187	0.646	0.726	0.797
CORAL 4E	0.517	0.011	43.219	3.748	0.004	22.327	0.033	0.126	0.029	0.010	48.544	12.240	0.632	0.646	0.674	0.754	0.797
GC-AZ	0.523	0.006	24.270	-14.484	0.011	3.045	0.004	-0.239	0.029	0.010	-2.157	-0.773	0.585	0.5312	0.554	0.634	0.724